ARCHIVES OF ACOUSTICS
28, 2, 71—91 (2003)

THE INFLUENCE OF THE SURFACE LOAD EXERTED BY A PIEZOELECTRIC CONTACT SENSOR ON TESTING RESULTS: I. THE DISPLACEMENT FIELD IN THE SOLID

L. RADZISZEWSKI

Kielce University of Technology
25-314 Kielce, Al. 1000-lecia P.P. 7, Poland

The influence of a strong discontinuity wave on its measurement with a piezoelectric sensor was analysed analytically. The one-dimensional model of the mechanical contact between the ultrasonic sensor and the solid medium was developed. The displacement field was calculated with the d'Alambert's method. The evaluation was made locally at the front of the distortion. It was found that the relative difference of a displacements between the free and loaded surfaces ranges from 10% to 72% and the mass M has no influence on it in the first time interval. It is affected not only by the wave impedances but also by the surfaces of the sensor and sample. After a long period of time (depending on the mass M) the influence of the surface loading becomes much smaller. Part I of the paper contains the discussion of the displacement field in the solid, the electrical transients generated by the piezoelectric sensor are given in Part II.

1. Introduction

Polymers and polymer composites are frequently used in mechanical systems (e.g. vehicle springs made of glass-fibre reinforced epoxy) because of their capacity of energy absorption and dissipation. Generally, they have viscoelastic and nonlinear properties, especially under the dynamic load, for instance the impingement.

In dynamic methods of investigation (e.g. resonance methods), the mechanical properties of these materials depend considerably on the measuring frequency at which they are determined. The quasi-static or ultrasonic testing is not sufficient to define the properties of such materials in the medium frequency range. The range corresponds to the frequencies observed in impact events. In viscoelastic materials we observe sudden frequency-dependent changes in the mechanical properties. Therefore, these properties should be measured continuously in the function of frequency using wide-band signals.

In this study we will focus our attention on the measuring methods where the material is in the form of a straight thin rod or a thick plate subjected to an impact or periodical load

occurring is the reason of wave's propagation. It may be of some significance to note that there exist two definitions of waves.

Any local impact or periodical excitation of particle motion can cause surface disturbances in the steady state of a solid.

In the case of an impact excitation, the distortion front (i.e. the displacement u, the displacement velocities v and strain ε) propagates in the medium from the impact-end with a velocity a. The front separates clearly the disturbed region of the material from the undisturbed one; this phenomenon is called the propagation of distortion waves (i.e. displacement-, strain- and stress waves). Across the front of the strain wave (and consequently the stress- and velocity wave) we can observe jumps in the value of ε or v, so the first derivatives of the displacement u with respect to t or to x are discontinuous [1]. These are the so-called waves of a strong discontinuity. At the front of the displacement wave u no such discontinuity is reported.

As elements of the medium are deformed periodically (or time-harmonically in a special case), the disturbances are transmitted from one point to the next one and the disturbances, or the wave, propagate through the solid also with the velocity a. But, the states (or phases) of motion are repeated periodically in space (every wavelength λ) and in time (every time period T), and $\lambda = aT$ where a is the phase wave velocity. In this situation it is not possible to indicate the wave front. The definition of discontinuity waves will be given further in this work.

LANZA di SCALEA in 1999 [2] has investigated by a noncontact laser method the influence of the surface load exerted by a piezoelectric contact transducer on the amplitude and frequency of vibrations making ultrasound pulse measurements in an aluminum plate. It has been reported that the contact transducer causes a 17% decrease in the amplitude of vibrations compared to those of the free surface. However, there is no evidence that the transducer affects the frequency characteristic of an optically measured signal.

The authors concluded that no effect of the particular piezoelectric transducer architecture on the ultrasonic wave propagation could be assessed. It could be possible by measurements in a steady state of the transducer.

In the measuring methods in rods, where the excitation has a time-harmonic character, the influence of the transducer mass on the results obtained is also analysed.

One end of the rod can be time-harmonically loaded and then the acceleration on both ends is measured. To enable a measurement of the accelerations, resonant vibrations should be excited in the rod, as suggested by NORRIS in 1970 [3]. PRITZ 1982 [4], on the other hand, proposed an excitation of vibrations in a wide range of frequency. ÖDEEN in 1993 [5] suggested that the above-mentioned method should be modified. The modification involved impact loading of one end and measuring accelerations with piezoelectric transducers on both ends.

It is interesting to note that in all these works a one-dimensional model of the phenomenon was assumed. To assure the correctness of the model [6], the wavelength has to be at least fivefold greater than the rod diameter (then the error caused by the inertia in the lateral direction will be less than 5%) and at least fivefold smaller than the rod length.

(because of the accuracy of determination of the moduli of elasticity of the material). Also, it has been reported that the mass of the sending and receiving transducers affects the rod vibration frequency characteristics.

BACON [7, 8] generated periodical distortions by irradiating the free end of a PVC- rod using short (i.e. 0.8 μs or 1.6 μs) rectangular microwave pulses at a small (585 Hz) frequency rate. The distortions were measured with a contact PZT transducer coupled to the other end of the rod. Two transducers with a mass of 0.65×10^{-3} kg and 11×10^{-3} kg were used in the test. The influence of the mechanical impedance of the transducer was taken into account in the presented theoretical one-dimentional model. This was confirmed experimentally. The amplitude of the acceleration measured by a transducer with a mass of 0.65×10^{-3} kg is nearly twice as great as that measured by a transducer with a mass of 11×10^{-3} kg. The results obtained by both transducers were compared and it has been found that the discrepancy between the experimental and theoretical results for the transducer with a mass of 11×10^{-3} kg is greater than for the transducer with a mass of 0.65×10^{-3} kg.

The authors, however, did not take into account the fact that the transducers applied in the experiments differed in the inside and outside structure (dimensions, material), which might have affected the results. It seems also that the relation of transducer's (11×10^{-3} kg) to the test specimen mass is too high (about 20%) and the accuracy of the measurements decreases.

Let us assume that the acoustic source induced by the impact method is a point source. Then, the emitted waves have spherical front surfaces. POUET in 1993 [9] observed that the effect of the geometric divergence depends on a constant correction factor ln3 and is independent of the thickness and the frequency. The phase velocity is not altered by the geometric divergence (independent of the plane wave or spherical wave hypotheses).

When propagating in the rod, they will be reflected by the sides, which will lead to the wave transformation. The reflected waves interfere with one another and as the result different wave modes with complex surfaces are generated.

KWUN confirmed this in 1993 [10]. His investigations concerned the propagation of a distortion generated by breaking a 0.5 mm pencil lead on the front surface of the rod 3.6 m in length and using two transducers (i.e. a piezoceramic one and a magnetostriction one). The latter, that is sensitive to stress waves, indicated the presence of a longitudinal wave only. Apart from the distortion caused by the arrival of a longitudinal wave, the piezoelectric transducer indicated the presence of other waves that were identified by the authors as a torsional wave mode.

However, since the dilatation wave propagates with a much greater velocity than the other waves, the distortions can be differentiated and we can assume that the front of the longitudinal wave reaches the measuring transducer first.

The authors, however, did not indicate to which physical parameter of the distortion the piezoelectric sensor is sensitive. Signals generated by longitudinal waves in this two different sensor were compared. The sensors were one by one but not exactly in the same position. The beginning of the signals in time interval from 0.1 ms to 0.5 ms were analysed but the wave's surfaces were not differentiated. Based on the data shown in this paper

(frequency, amplitude, attenuation) it is concluded that the signals measured by both the transducers, PZT and EMAT, are almost the same. It means also that the presence of a coupling layer by measurements of a transient distortion with a PZT transducer does not change the measured signals significantly.

The studies quoted above deal with a wave generation by periodical pulse- or time-harmonic methods in different materials and of different forms. The aim was to determine their mechanical properties – elastic or unelastic. A piezoelectric transducer coupled on the rod was used for the measurements. The transducer was assumed to be a rigid mass of known mechanical impedance.

Because of the differences in the material properties of the medium and the transducer, the surface displacement in the absence of the sensor is not exactly the same as the sensor displacements. Since it is the goal of measuring devices to obtain values for the wave field that would exist if no device were present, we would like to analyse this problem once more but in another way. Contrary to the previous authors we would like to investigate the influence of the sensor load on the displacement field generated by transient disturbance in the measured solids. The sensor is assumed to be a continuous mass.

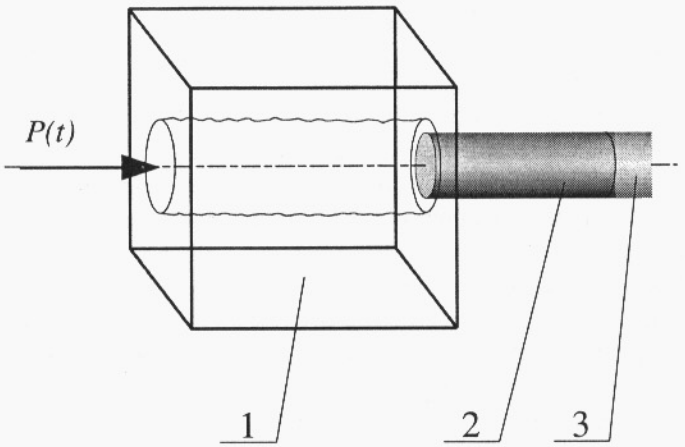

Fig. 1. Schematic model of the specimen and the probe; 1–specimen, 2–transducer, 3–seismic mass.

We could virtually cut from the analysed specimen, a symmetric figure which one dimension in the direction of the symmetry axis (longitudinal) is much greater than that in the perpendicular ones. We can ommit the strains in the perpendicular directions. Let the wave's front of the disturbances generated by a point source on the front surface of the rod be spherical ones. We can assume that on the area equal to the perpendicular cross-section of the rod, the shape of wave's surface is plain. Then, we could say that in this virtually rod propagates in the longitudinal direction a disturbance with the velocity of a longitudinal wave and with a plain wave's surface. We assume that the material of the rod is

homogenous and the characteristic stress as function of strain is nonlinear like in a viscoelastic material. In this work we assume also that the strains are in a linear elastic range. So we will analyse the propagation of disturbances in a one- dimensional linear elastic material. Let us expand now the strong discontinuity wave into a series of soft discontinuity waves. The velocities of the strong and soft discontinuity waves in such a material are equal. Because we are going to continue this analysis also for strains, which are not elastic linear, in order to keep the same notation and names, we call our disturbances as waves of strong discontinuity. We would like to focus on some essential physical aspects of the problem, and therefore the mathematical analysis is simplified, because one-dimensional geometry with a plane incident wave is considered. We shall analyse the longitudinal vibration locally on the face of the disturbances.

First, the aim of the current paper is to predict the influence of the sensor load on the displacement field in the solid (Part I). An axial local impact causes the propagation of distortion waves in a rod. We would analyse the propagation of the transient distortion locally, i.e. at the front [11].

Afterwards, we shall analyse the influence of a strong discontinuity wave on its measurement with a piezoelectric sensor theoretically. When the distortion front arrives the measuring sensor coupled at the back face of the rod, electrical transients will be generated from the piezoelement. In the case of a piezoceramic transducer, it is worthy analysing how it will behave when a strong discontinuity wave is incident on it and what quantity we shall obtain as a response (Part II).

2. Model of the mechanical contact between the ultrasonic sensor and the solid medium

Let us consider a short impact excitation with a time duration τ in the rod. A force $P(t)$ is applied to the front surface of the rod located at the point $x = 0$, whereas the back face (at the point $x = L$) is loaded with a measuring piezoelectric sensor (Fig. 2). The force $P(t)$ has the character of a step function with the value P_0. The longitudinal vibrations of the rod are described by the wave propagation equation $\frac{\partial^2 u(x,\ t)}{\partial t^2} - a^2 \frac{\partial^2 u(x,\ t)}{\partial x^2} = 0$, where $a = \sqrt{\frac{E}{\rho}}$ is the velocity, E – the Young's modulus, ρ – the rod material density. We assume the solution of this wave equation in the d'Alembert's form [11] $u(x, t) = f_1(at - x) + f_2(at + x)$.

Figure 2b shows the characteristics on the plane (x, t) of the impact pulse traveling along the rod. Having traveled the whole distance corresponding to the rod length L (rod 1), the pulse is reflected. After each reflection from the back surface going through the point $x = L$, a part of the energy travels to the transducer (rod 2) in accordance with the Snell's law of reflection. We can assume that in the transducer (regions for $x \in [L,\ L + h]$) an analogous phenomenon of subsequent reflections occurs. The only difference is that we do not observe the energy transfer through the surface $x = L + h$, which is assumed to be rigidly loaded with

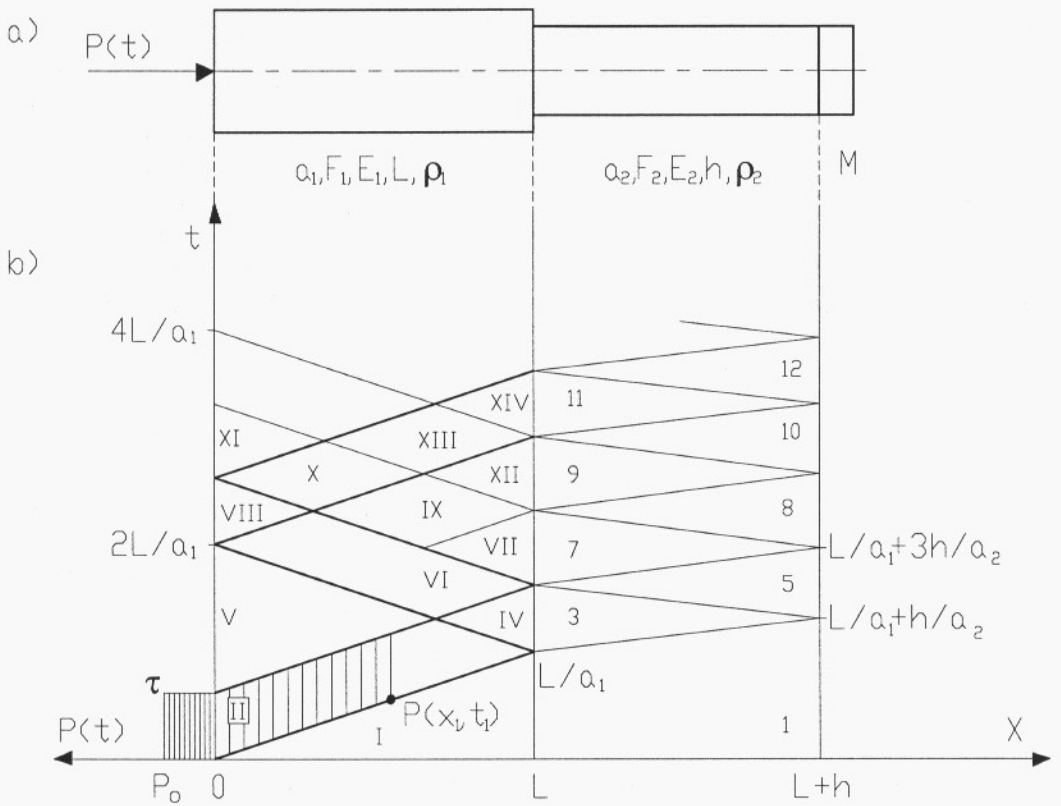

Fig. 2. Model of a solid medium and a piezoelectric sensor (2a) and the wave fronts in the analyzed rod and sensor (2b).

the mass M of a density much greater than the density ρ_2 of rod 2. The sections of the characteristic between the subsequent pulse reflections in the rod divide a part of the plane (x, t) for $0 \le x \le L$ into regions designated by Roman numerals of consecutive numbers. In a similar fashion, the sections of the characteristic between the subsequent pulse reflections in the transducer divide a part of the plane (x, t) for $L \le x \le L+h$ into regions designated by Arabic numerals of consecutive numbers. Also, we assume that the impact pulse falls and is reflected always in the direction normal to the rod face surfaces ($x = 0$ or $x = L$ or $x = L + h$). Since there is no conversion of the waveform (no shear waves), the distortion energy propagates only in the form of a longitudinal wave and the displacements are observed only along the rod axis (Fig. 2a). The pulse width τ of the impulse can be very short but long enough to exite the rod to vibration. The problem will be solved analitycally. We assume that $\tau = \frac{2}{3}\frac{L}{a_1} = \frac{2h}{a_2}$ but for any other value of τ our consideration will be still valid. Only the density of the characteristics on the plane (x, t) will be changed.

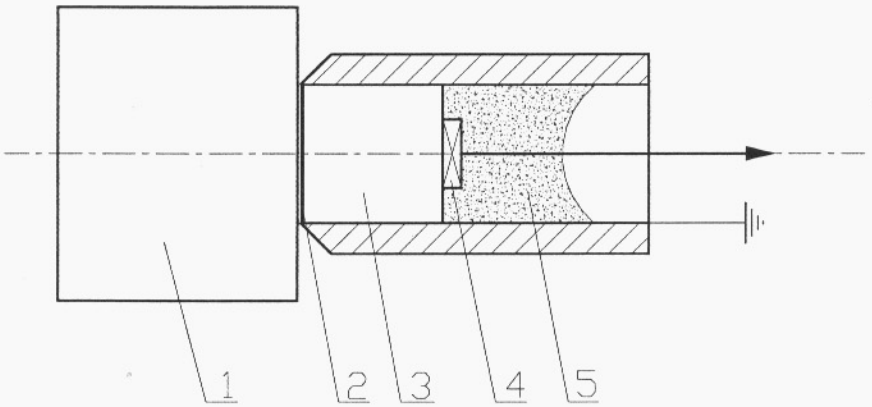

Fig. 3. Cross-section of a broadband ultrasonic probe; 1 – sample, 2 – couplant, 3 – buffer, 4 – piezoelectric transducer, 5 – seismic mass [12].

The architecture of the broadband ultrasonic probe (shown in Fig. 3) is much more complicated than our model. The acoustic impedance of the piezoelectric transducer is often much greater than the impedance of the investigated medium. This is the reason why we should use a couplant layer and one or more impedance- matching front layers or a buffer between the sample and the probe.

The thickness of these matching layers should be equall to $(2n + 1)\frac{\lambda_{el}}{4}$, where n – number, λ_{el} – wave's length calculated for the frequency of the electrical resonance of the transducer [13].

On the bondaries between the specimen and the coupling and matching layers, there is the greatest acoustical impedance mismatch. The changes of the thickness of these layers are the main source of errors in the ultrasound contact measurements.

In the case of measurements of transient signals with a contact piezoelectric transducer, the influence of coupling and matching layers should be less important.

The measured signal propagates in these layers only once. Let's assume that the thicknesses of these layers are sufficiently small, so we can ommit the wave's energy losses during propagation. The reverberation also do not take place. The loading effect of these layers is still present but we can take it into account by enlarging a little the seismic mass. Because of those reasons, these layers are not drawn in our model of the transducer in Fig. 2a.

In the region I (Fig. 2b) we solve the Cauchy's problem for the data along the axis $t = 0$. If, for instance, we focus our attention on the point $P(x_1, t_1)$ in the first section of the characteristic with the equation $a_1 t - x = 0$, we can say the distortion face front goes through the point x_1 at the moment t_1, i.e. for $x > x_1$ we observe $u_I(x, t) = 0$ (no strain caused by the distortion). We will write the displacement as follows: $u_I(x, t) = f_1(a_1 t - x) + f_2(a_1 t + x)$, where a_1 is the wave velocity in the rod 1. We assume that the initial conditions are zero, i.e.

for the time $t = 0$ the displacement $u_I(x, 0) \equiv 0$ and the velocity $\frac{\partial u_I(x, t)}{\partial t} \equiv 0$. We obtain the following relationships: the displacement $u_I(x, 0) = f_1(-x) + f_2(x) = 0$, and the velocity $\frac{\partial u_I(x, t)}{\partial t}_{t=0} = a_1 f_1'(-x) + a_1 f_2'(x) = 0$. Differentiating $u_I(x, 0)$ in relation to x we get the strain $-f_1'(-x) + f_2'(x) = 0$ and, from the condition $\frac{\partial u_I(x, t)}{\partial t} = 0$ for $t = 0$, we get the velocity $f_1'(-x) + f_2'(x) = 0$. Solving the above equations yields $f_1'(-x) = 0$ and $f_2'(x) = 0$. Since the above considerations are valid for $x \geq 0$, the function $f_1'(\ )$ is for the negative and zero arguments equal to zero and the function $f_2'(\ )$ is equal to zero for positive arguments. The value $f_1'(\ )$ for positive arguments cannot be determined from the initial conditions only. Taking into account the above equations we can write $f_1(-x) = C_1 = \text{const}$, and $f_2(x) = C_2 = \text{const}$. The condition $u_I(x, 0) = f_1(-x) + f_2(x) = C_1 + C_2 = 0$ yields $C_1 = -C_2$. Denoting $C_2 = C$ we obtain $f_1(-x) = -C, f_2(x) = C$, where the variable x plays the role of an argument of the functions $f_1(\ ), f_2(\ )$ in these equations. Thus, the results can be generalised and written as $f_1(a_1 t - x) = -C$ for $a_1 t - x \leq 0$; whereas $f_2(a_1 t + x) = C$. Hence the solution for the displacement is $u_I(x, t) = f_1(a_1 t - x) + f_2(a_1 t + x) = -C + C = 0$. However, this solution is valid only for $a_1 t - x \leq 0$, so it is valid in a region on the plane (x, t) limited by the above inequality. The region was shown in Fig. 2b (region I). Therefore, we have obtained only the solution in the region I, in which

$$u_I(x, t) \equiv 0 \quad \text{and accordingly} \quad v_I(x, t) = \frac{\partial u_I(x, t)}{\partial t} \equiv 0, \quad \varepsilon_I(x, t) = \frac{\partial u_I(x, t)}{\partial x} \equiv 0. \tag{1}$$

The solution of the wave propagation equation for the displacement in the region II (Fig. 2b) can be written as follows: $u_{II}(x, t) = f_1(a_1 t - x) + f_2(a_1 t + x)$. On the characteristic $a_1 t - x = 0$ we have $u_I(x, t) = 0$, then assuming the continuity of displacements on this characteristic, we must have $u_{II}(x, t) = 0$ as well. Hence substituting $a_1 t - x = 0$ yields $u_{II}(x, t) = f_1(0) + f_2(2a_1 t) = 0$, and after a simple transformation $f_2(2a_1 t) = -f_1(0) = \text{const}$. Substituting $2a_1 t = \chi$ and differentiating on both sides yields $f_2'(\chi) = -f_1'(0) = 0$. After the double-sided integration and introducing the notation $\chi = a_1 t + x$ we can write $f_2(a_1 t + x) = -f_1(0) = \text{const}$. The solution $u_{II}(x, t)$ in the region II should satisfy the boundary condition for $x = 0$. The condition results from the loading of the rod 1 with a pulse force $P(t)$ rectangular in time (Fig. 2b). The force will cause a stress $\partial_{II}(0, t) = -\frac{P(t)}{F_1}$ and a strain $\varepsilon_{II}(0, t) = \frac{\partial u_{II}(0, t)}{\partial x} = -\frac{P(t)}{E_1 F_1}$, where E_1 stands for the Young's modulus and F_1 is the surface area of the front (and back) face of the rod 1. Hence, on the boundary $x = 0$ we have the strain

$\varepsilon_{II}(0,t) = \dfrac{\partial u_{II}(0,t)}{\partial x} = -f_1'(a_1 t) + f_2'(a_1 t) = -\dfrac{P(t)}{E_1 F_1}$ for $t > 0$. Substituting $a_1 t = \delta$ we get $-f_1'(\delta) + f_2'(\delta) = -\dfrac{P(\delta/a_1)}{E_1 F_1}$. After transformation, the equation can be written in the following form $f_1'(\delta) = \dfrac{P(\delta/a_1)}{E_1 F_1} + f_2'(\delta) = \dfrac{P(\delta/a_1)}{E_1 F_1}$. After double-sided integration and the introduction of the notation $\delta = a_1 t - x$, we get $f_1(a_1 t - x) = \int_0^{a_1 t - x} \dfrac{P(\delta/a_1)}{E_1 F_1}\, d\delta + f_1(0)$.

The solution for the displacement in the region II can be as follows

$$u_{II}(x,t) = f_1(a_1 t - x) + f_2(a_1 t + x) = \int_0^{a_1 t - x} \frac{P(\delta/a_1)}{E_1 F_1}\, d\delta. \tag{2}$$

The solution obtained is valid in the region II limited also by the characteristic $a_1 t + x = 2L$. In the region to the right of it, i.e. region IV, the condition is that a measuring sensor has been placed on the right end of the rod 1. A model of such a sensor in the form of rod 2 with the length h and loading mass M is presented in Fig. 2a. It is assumed that the loading mass M is a rigid bar with a density much greater than the density of the investigated material or the material of the transducer, e.g. quartz or PZT ceramic. In a similar way as for region II, we will determine the solutions in regions IV, 3, 5 (details are provided in Appendix). It is assumed that on the characteristics, the equality and continuity of the displacements are observed.

Let us assume that in the boundary surface area, for $x = L$, between the rod 1 and the sensor we have the equality of displacements and the following equation is satisfied:

$$\varepsilon_{IV}(x,t) E_1 F_1 = \varepsilon_3(x,t) E_2 F_2.$$

The displacement for the region 3 can be written as

$$u_3(x,t) = \frac{2a_1}{(a_2 + \alpha a_1) E_1 F_1} \int_{L\frac{a_2 - a_1}{a_1}}^{a_2 t - x} P\left(\frac{a_1 \beta + L(a_1 - a_2)}{a_1 a_2}\right) d\beta \tag{3}$$

where $\alpha = \dfrac{E_2 F_2}{E_1 F_1}$, E_2 – Young's modulus and F_2 – the surface area of the front face of the rod 2.

The displacement in the region IV is

$$u_{IV}(x,t) = \int_0^{a_1 t - x} \frac{P(\delta/a_1)}{E_1 F_1}\, d\delta + \frac{a_2 - a_1\alpha}{(a_2 + \alpha a_1) E_1 F_1} \int_{2L}^{a_1 t + x} P\left(\frac{\eta - 2L}{a_1}\right) d\eta. \tag{4}$$

The displacements in regions II, IV and 3 could be calculated of for any force $P(t)$ from equations (2), (3), (4) in a simple way. In the next regions such calculations for any given force $P(t)$ is much more complicated. Because of this we can assume for simplicity that for $t \geq 0$ $P(t) = P_0 = \text{const}$.

Let us also assume that the wave falling on the interface with the co-ordinate $x = L + h$ is completely reflected (from the loading mass M). It is possible to write the formula for the displacement in the region 5 when the force $P(t) = P_0 = \text{const}$.

$$u_5(x,t) = \frac{4a_1 P_0}{(a_2 + \alpha a_1) E_1 F_1} \left(a_2 t - L\frac{a_2}{a_1} - h - \frac{M a_2^2}{E_2 F_2}\left[1 - e^{-k_1\left(\frac{a_2 t + x}{a_2} - \frac{L(a_1 + a_2)}{a_2 a_1} - \frac{2h}{a_2}\right)}\right]\right). \tag{5}$$

If the force $P(t) = P_0 = \text{const}$, the displacements of the ends of the rod 2 in the regions 3 and 5 can be written in the following form:

$$u_3(x,t) = \frac{2a_1 P_0}{(a_2 + \alpha a_1) E_1 F_1}\left[a_2 t - x - L\frac{a_2 - a_1}{a_1}\right], \tag{6}$$

in the cross-section $x = L$

$$u_3(L,t) = \frac{2a_1 P_0}{(a_2 + \alpha a_1) E_1 F_1}\left[a_2 t - L\frac{a_2}{a_1}\right], \tag{7}$$

and in the cross-section $x = L + h$

$$u_5(L + h, t) = \frac{4a_1 P_0}{(a_2 + \alpha a_1) E_1 F_1} \left(a_2 t - L\frac{a_2}{a_1} - h - \frac{M a_2^2}{E_2 F_2}\left[1 - e^{-k_1\left(t - \frac{L}{a_1} - \frac{h}{a_2}\right)}\right]\right). \tag{8}$$

The displacements in the remaining regions were determined according to the described methodology and the calculation results are given in the Appendix.

3. Influence of the sensor load on the displacement field in the solid

Let us compare the displacement of the free right end (with the co-ordinate $x = L$) of the rod 1 with the displacement obtained when the end is loaded with various contact sensors (Figs. 4 and 5). The comparison will be made in the region IV for the time $t \in < L/a_1, L/a_1 + 2h/a_2 >$ and then in the regions VII and XII for the time $t \in < L/a_1 + 2h/a_2, L/a_1 + 6h/a_2 >$. The displacement of the free right end of this rod is determined by the following relationship

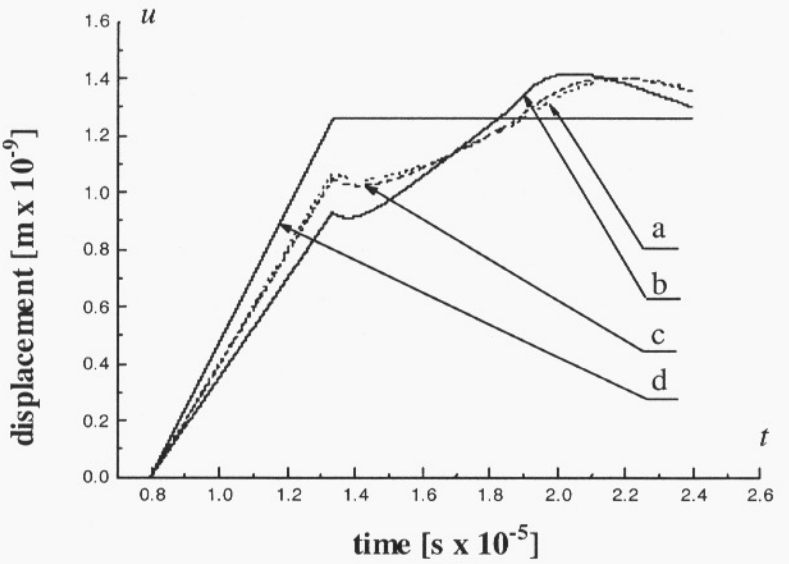

Fig. 4. Displacement of the back face of an aluminum rod as function of time loaded with a) a quartz sensor, b) a PZT sensor, c) an aluminum cylinder, or d) free, loading mass $M = 2 \times 10^{-3}$ kg.

$u(L, t) = \dfrac{2P_0(a_1 t - L)}{E_1 F_1}$. The formula defining the displacement $u_{IV}(L, t)$ of the same loaded end of the rod was given above (4). Now let us determine the ratio of both displacements

$$\varphi = u_{IV}(L, t)/u(L, t) = \frac{a_2}{a_2 + a_1 \dfrac{E_2 F_2}{E_1 F_1}} \leq 1.$$

From this relationship it is clear that the displacement of the rod end loaded with a sensor is always smaller than that of the free one. It should be noted that these relationships (valid for region IV) do not include the loading mass M but they include the Young's modulus, the transducer material density and contact area. The mass M has no influence in the time interval analysed because the evaluation is made locally at the front of the distortion wave. Let us determine the relative

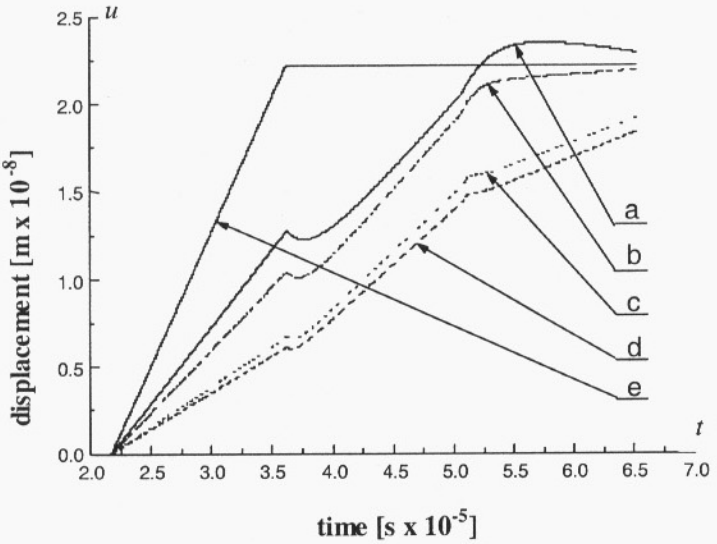

Fig. 5. Displacement of the back face of rod 1 made of PVC in the time function loaded with; a) a $LiSO_4$ sensor, b) a quartz sensor, c) a PZT ceramic sensor, d) a $LiNbO_3$ sensor, or e) free, loading mass $M = 2\times10^{-3}$ kg.

difference between the displacements (relative error) $\frac{\Delta u}{u(L,t)} = \frac{u(L,t) - u_{IV}(L,t)}{u(L,t)}$

$= \frac{\alpha a_1}{a_2 + \alpha a_1}$. The relationship determining the parameter φ can be transformed as

$\varphi = \frac{1}{1 + \frac{a_2\rho_2 F_2}{a_1\rho_1 F_1}} = \frac{1}{1 + \frac{Z_2 F_2}{Z_1 F_1}}$, where $Z_i = a_i\rho_i$ for $i = 1, 2$. For the considered case of a plain wave, Z_i is the wave impedance of the rod –1 or –2. Let us write the relative difference between the displacements using the concept of wave impedance $1 - \varphi = \frac{Z_2 F_2}{Z_1 F_1 + Z_2 F_2}$.

It is clear that the relative difference between the displacements is affected not only by the wave impedance but also by the sensor and sample area F_i. After a longer period of time, when the wave has been reflected from the interfaces several times, the influence of the mass M will be evident.

In Ref. [2], the measuring error of the amplitude (for an aluminum plate) was determined experimentally with a PZT transducer and found to be 17%. In this study, the authors [2] replaced the receiving transducer with an appropriate aluminum cylinder and found that there was no difference neither in the amplitude nor in the frequency of the received signal. The experiment shows that the structure of the transducer does not affect the received signal. However, the conclusion cannot be regarded as absolutely true. The calculations performed according to the model proposed demonstrate that also for

aluminum the relative difference between the displacements in the region IV is 26% for the PZT sensor, 15% for the quartz sensor and 17% for the aluminum cylinder. For a PVC sample and a quartz sensor the difference is 53% and for the PZT sensor 70%. In the next regions, i.e. VII and XII for the time $t \in < L/a_1 + 2h/a_2, L/a_1 + 6h/a_2 >$, the influence of the mass M is more noticeable (Fig. 4 and Appendix). The relative difference between displacements of 17% for the aluminum-PZT sensor is observed for the time $t = 1.6 \times 10^{-5}$, as shown in Fig. 4. If we replace the PZT sensor with an aluminum cylinder, then for the time $t = 1.6 \times 10^{-5}$, the relative difference between displacements is approximately – 14% (Fig. 4). Comparing the results presented in Ref. [2] with those obtained by the author for the aluminum / aluminum cylinder, one can conclude that the results in the suggested theoretical model are overestimated by about 3%. This may be due to the fact that in the model, the analysis concerns local changes at the distortion front whereas in the experimental study we frequently deal with averaged values.

Comparing Fig. 4 and Fig. 5 we can say that the displacements' field in the rod 1 depends on the kind of the transducer coupled to his back face.

When measuring the displacements of the back faces loaded with a transducer, there always exists a systematic error. This error for different transducers are compared in Table 1. The greatest error in the measurements of the amplitude of displacements or velocity in a PVC sample, in region IV in Fig. 2, is for transducers made of $LiNbO_3$ and $BaTiO_3$, the smallest one for $LiSO_4$. Though these transducers are rarely used because of different reasons.

We should point out that a quarz transducer goes to a steady state of equlibrium (Fig. 5) in the shortest time.

We could say, that a PZT transducer causes a great measuring error but they reach the steady state of equlibrium in almost the same time as the $LiNbO_3$ transducer.

In Table 1, there are two transducers made of a PZT ceramic of a little different material properties that results in differences of 2% in the measuring error. In next regions the influence of the material of the transducer on the measuring error is much smaller.

Table 1. Parameters of piezoelectric materials and measuring error in a PVC or aluminum rod.

Piezoelectric material	Density $\rho_2[\times 10^3$ kg/m$^3]$	Velocity of longitudinal wave $a_2[\times 10^3$ m/s]	Measuring error in aluminum $(1\text{-}\varphi)_{Al}$ [%]	Measuring error in PVC $(1\text{-}\varphi)_{PVC}$ [%]
PZT	7.75	3.88	26	70
PZT 5A	7.75	4.35	28	72
Quartz	2.65	5.57	15	53
$BaTiO_3$	5.70	5.47	27	71
$LiNbO_3$	4.65	7.35	29	72
$LiSO_4$	2.06	4.72	10	43
Pb Nb_2O_0	5.80	2.80	16	56

4. Final remarks and conclusions

Let us summarize the simplifying assumptions which restrict the validity of the results presented here. The assumptions are:

1) deformations in the linear-elastic region,
2) one-dimensional model of the transducer,
3) the analysis concerns local changes at the plain front of the distortion,
4) the impact pulse falls and is reflected always in the direction normal to the rod interfaces,
5) there is no energy transfer through the interface between the material of the transducer and the mass M,
6) load of the rod with an impulsive force $P(t)$ rectangular in time.

On the basis of the results of the above calculations one can conclude that the intrusive influence of the contact transducer on the displacement field in tested specimens is extremely important in the initial period of time after the distortion occurs. The mass M has no influence on the displacements in the first analysed time interval because the evaluation is made locally at the front of the distortion wave. The relative difference between the displacements is affected not only by the wave impedances but also by the surfaces of the transducer and the sample. Depending on the type of the sample and the transducer applied, this differences range from 10% to 72%, and therefore they are of great significance. But there are systematic errors. Such errors are not so difficult to compensate by an analysis of the results. After few reflections in the next regions, the influence of surface loading becomes smaller and after a long period of time (depending on the value of the loading mass M) is rather negligible. This is the reason of the popular opinion that by time-harmonic waves the influence of surface loading with a transducer is not important. Although, after a long period of time and after multiple reflections different wave modes with complex surfaces are present in the signals which causes other problems in the analysis of the results.

Appendix

Applying the d'Alembert's solution of the wave propagation equation, the displacement in the region 1 (Fig. 2b) can be written as $u_1(x, t) = g_1(a_2 t - x) + g_2(a_2 t + x) = 0$ where a_2 is the wave velocity in the rod 2. We assume that on the characteristic $x = a_2(t - L/a_1) + L$ the equality and continuity of displacements $u_1(x, t) = u_3(x, t)$ are observed. The displacement in the region 3 can be expressed in the following form: $u_3(x, t) = g_1(a_2 t - x) + g_2(a_2 t + x)$. Applying the equation of the characteristic, the formula becomes $g_1\left[L\left(\frac{a_2}{a_1} - 1\right)\right] + g_2\left[2a_2 t + L\left(1 - \frac{a_2}{a_1}\right)\right] = 0$. Let us introduce the

notation $2a_2 t + L\left(1 - \frac{a_2}{a_1}\right) = \kappa$. Now we can write $g_2(\kappa) = -g_1\left[L\left(\frac{a_2}{a_1} - 1\right)\right] = \text{const.}$

Then, after differentiating and inserting $\kappa = a_2 t + x$ we get

$$g_2(a_2 t + x) = -g_1\left[L\left(\frac{a_2}{a_1} - 1\right)\right] = \text{const.} \tag{A1}$$

It is assumed that on the characteristic $x + a_1 t = 2L$ the equality of displacements occurs $u_{II}(x, t) = u_{IV}(x, t)$.

$$u_{IV}(x, t)_{x=-a_1 t+2L} = f_1(2a_1 t - 2L) + f_2(2L) = \int_0^{2a_1 t - 2L} \frac{P(\delta/a_1)}{E_1 F_1}\, d\delta.$$

Let us introduce the notation $2a_1 t - 2L = \varphi$. We can write $f_1(\varphi) = \int_0^{\varphi} \frac{P(\delta/a_1)}{E_1 F_1}\, d\delta - f_2(2L)$.

Substituting $\varphi = a_1 t - x$ yields

$$f_1(a_1 t - x) = \int_0^{a_1 t - x} \frac{P(\delta/a_1)}{E_1 F_1}\, d\delta - f_2(2L). \tag{A2}$$

Let us assume that on the interface between the rod and the transducer for $x = L$ we observe the equality of displacements and the equation $\varepsilon_{IV}(x, t) = \alpha\varepsilon_3(x, t)$ is satisfied, where $\alpha = \frac{E_2 F_2}{E_1 F_1}$, E_2 and F_2 are the Young's modulus and the cross-sectional area of the rod 2 respectively. From the above considerations we know that the strains can be written as:

$$\varepsilon_{IV}(x, t) = -f_1'(a_1 t - x) + f_2'(a_1 t + x)$$

$$\varepsilon_3(x, t) = -g_1'(a_2 t - x) + g_2'(a_2 t + x)$$

After replacing the above expressions with the function derivatives f_1', f_2', g_1', g_2' we obtain

$$f_2'(a_1 t + L) = \frac{1}{E_1 F_1} P\left(\frac{\alpha_1 t - L}{a_1}\right) - a g_1'(a_2 t - L) \tag{A3}$$

Let us introduce the notation $a_1 t + L = \eta$. Hence we have $a_1 t - L = \eta - 2L$. Let us assume that on the boundary surface of the regions IV and 3, for $x = L$, an equality of velocity is observed and after transforming it we obtain

$$f_2'(a_1 t + L) = \frac{a_2}{a_1} g_1'(a_2 t - L) - \frac{1}{E_1 F_1} P\left(\frac{a_1 t - L}{a_1}\right). \tag{A4}$$

Hence we shall determine, $f_2'(a_1 t + x)$ and $g_1'(a_2 t - x)$. After a little manipulation this equation can be written as follows $g_1'(a_2 t - L) = \frac{2a_1}{(a_2 + \alpha a_1)\ E_1 F_1} P\left(\frac{a_1 t - L}{a_1}\right)$. On introducing the notation $a_2 t - L = \beta$ and integrating, the above equation yields

$$g_1(\beta) = \frac{2a_1}{(a_2 + \alpha a_1)\ E_1 F_1} \int_0^{\beta} P\left(\frac{a_1 \beta + L(a_1 - a_2)}{a_1 a_2}\right) d\beta + W \tag{A5}$$

where W is the integration constant. For $\beta = a_2 t - x$, the equations (A1) and (A5) become

$$g_1(a_2 t - x) = \frac{2a_1}{(a_2 + \alpha a_1)\ E_1 F_1} \int_0^{a_1 t - x} P\left(\frac{a_1 \beta + L(a_1 - a_2)}{a_1 a_2}\right) d\beta + W,$$

$$g_2(a_2 t + x) = -\, g_1\left[L\left(\frac{a_2}{a_1} - 1\right)\right] = \tag{A6}$$

$$\frac{-2a_1}{(a_2 + \alpha a_1)\ E_1 F_1} \int_0^{L\frac{a_2 - a_1}{a_1}} P\left(\frac{a_1 \beta + L(a_1 - a_2)}{a_1 a_2}\right) d\beta - W.$$

The displacement for the region 3 and the characteristic $a_2\left(t - \frac{L}{a_1}\right) + L = x$ can be written as

$$u_3(x, t) = \frac{2a_1}{(a_2 + \alpha a_1) E_1 F_1} \int_{L\frac{a_2 - a_1}{a_1}}^{a_2 t - x} P\left(\frac{a_1 \beta + L(a_1 - a_2)}{a_1 a_2}\right) d\beta. \tag{A7}$$

From equations (A3) and (A5), after simple transformations and integrations, we become

$$f_2(\eta) = \frac{1}{E_1 F_1} \int_{2L}^{\eta} P\left(\frac{\eta - 2L}{a_1}\right) d\eta - \frac{2a_1 \alpha}{(a_2 + \alpha a_1)\ E_1 F_1} \int_{2L}^{\eta} P\left(\frac{\eta - 2L}{a_1}\right) d\eta. \tag{A8}$$

Introducing the notation $\eta = a_1 t + x$ we get

$$f_2(a_1 t + x) = \frac{a_2 - a_1\alpha}{(a_2 + \alpha a_1)\ E_1 F_1} \int_{2L}^{a_1 t + x} P\left(\frac{\eta - 2L}{a_1}\right) d\eta. \tag{A9}$$

The displacement in the region IV is

$$u_{IV}(x, t) = \int_0^{a_1 t - x} \frac{P(\delta/a_1)}{E_1 F_1} d\delta + \frac{a_2 - a_1\alpha}{(a_2 + \alpha a_1)\ E_1 F_1} \int_{2L}^{a_1 t + x} P\left(\frac{\eta - 2L}{a_1}\right) d\eta. \tag{A10}$$

We assume that on the boundary of regions 3 and 5 a continuity and the equality of displacements are observed, $u_5(x, t) = u_3(x, t)$. Let us express the displacement in the region 5 as $u_5(x, t) = h_1(a_2 t - x) + h_2(a_2 t + x)$. The displacement on characteristic $x = -a_2(t - L/a_1) + L + 2h$ between regions 3 and 5 can be written as

$$u_5(x, t) = h_1\left[2a_2 t - L\left(1 + a_2/a_1\right) - 2h\right] + h_2\left[L\left(1 + a_2/a_1\right) + 2h\right].$$

On introducing the notation $\theta = 2a_2 t - L\left(1 + a_2/a_1\right) - 2h$ and after a little manipulation we can write $h_1'(\theta) = \dfrac{2a_1}{(a_2 + \alpha a_1)\ E_1 F_1} P\left[\dfrac{a_1\theta + L(a_1 - a_2)}{a_1 a_2}\right]$. Hence, for $\theta = a_2 t - x$ we obtain

$$h_1(a_2 t - x) = \frac{2a_1}{(a_2 + \alpha a_1) E_1 F_1} \int_{L\frac{a_2 - a_1}{a_1}}^{a_2 t - x} P\left(\frac{a_1\beta + L(a_1 - a_2)}{a_1 a_2}\right) d\beta$$

$$- h_2\left[L\left(1 + \frac{a_2}{a_1}\right) + 2h\right]. \tag{A11}$$

It is assumed that the wave falling upon the surface with the co-ordinate $x = L + h$ is completely reflected (from the loading mass M). Let us consider the equation of equilibrium of the forces acting upon the mass M (Fig. A1); the force $F_2\sigma_5$ can be expressed as

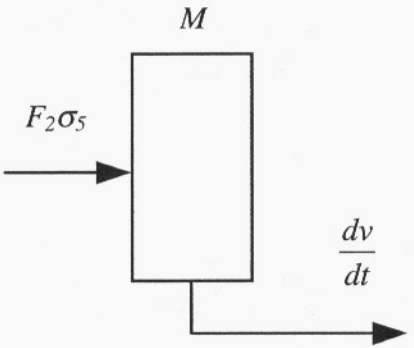

Fig. A1. Schematic diagram of forces acting upon the loading mass M.

$$E_2F_2\frac{\partial u_5(x,t)}{\partial x} = {}_{x=L+h} = E_2F_2\left[-h_1'(a_2t - L - h) + h_2'(a_2t + L + h)\right]. \quad \text{(A12)}$$

The equation of equilibrium of the forces acting upon the mass M is

$$E_2F_2\frac{\partial u_5(x,t)}{\partial x} + M\frac{\partial v(t)}{\partial t} = {}_{x=L+h} = 0, \quad \text{(A13)}$$

$$v(t) = \frac{\partial u_5(x,t)}{\partial t} = {}_{x=L+h} = a_2h_1'(a_2t - x) + a_2h_2'(a_2t + x).$$

After a simple transformation, the velocity of the mass M for $x = L + h$ is

$$h_2'(a_2t + L + h) = \frac{1}{a_2}v(t) - h_1'(a_2t - L - h).$$

Let us rewrite the equation of equilibrium of the forces acting upon the mass M

$$\frac{dv(t)}{dt} + v(t)\frac{E_2F_2}{Ma_2} = \frac{2}{M}h_1'(a_2t - L - h)E_2F_2. \quad \text{(A14)}$$

From the above calculations it is clear that

$$h_1'(a_2t - L - h) = \frac{2a_1}{(a_2 + \alpha a_1)\ E_1F_1}P\left[t - \frac{L}{a_1} - \frac{h}{a_2}\right]. \quad \text{(A15)}$$

Let us assume the notation $\frac{1}{M}\frac{E_2F_2}{a_2} = k_1$ and that the force $P(t) = P_0 = \text{const}$. Then, the equation of equilibrium of forces acting upon the mass M can be finally written as

$$\frac{dv(t)}{dt} + v(t)\,k_1 = {}_{x=L+h} = \frac{2}{M}\frac{2a_1E_2F_2}{(a_2 + \alpha a_1)E_1F_1}P_0. \tag{A16}$$

Let us assume the precondition $v\left(\frac{L}{a_1} + \frac{h}{a_2}\right) = 0$.

Solving the above non-homogeneous differential equation yields

$$v(t) = \frac{4a_1P_0}{a_2 + \alpha a_1}\frac{a_2}{E_1F_1}\left[1 - e^{-k_1\left(t - \frac{L}{a_1} - \frac{h}{a_2}\right)}\right]. \tag{A17}$$

From the above expression we shall determine $h_2'(a_2t + x)$ for $x = L + h$ and obtain

$$h_2'(a_2t + L + h) = \frac{4a_1}{a_2 + \alpha a_1}P_0\frac{1}{E_1F_1}\left[1 - e^{-k_1\left(t - \frac{L}{a_1} - \frac{h}{a_2}\right)}\right] - h_1'(a_2t - L - h). \tag{A18}$$

Let us introduce the notation $\xi = a_2t + L + h$. Transforming the above dependence yields

$$h_2'(\xi) = \frac{2a_1P_0}{(a_2 + \alpha a_1)\,E_1F_1} - \frac{4a_1}{a_2 + \alpha a_1}\frac{P_0}{E_1F_1}e^{-k_1\left(\frac{\xi}{a_2} - \frac{L(a_1+a_2)}{a_1} - \frac{2h}{a_2}\right)}. \tag{A19}$$

After double-sided integration we obtain

$$h_2(\xi) = \frac{2a_1P_0\xi}{(a_2 + \alpha a_1)\,E_1F_1} + \frac{4a_1}{a_2 + \alpha a_1}\frac{P_0}{E_1F_1}\frac{a_2}{k_1}e^{-k_1\left(\frac{\xi}{a_2} - \frac{L(a_1+a_2)}{a_2a_1} - \frac{2h}{a_2}\right)} + D, \tag{A20}$$

where D is the integration constant. Let us substitute the variable $\xi = a_2t + x$. We get

$$h_2(a_2t + x) = \frac{2a_1P_0(a_2t + x)}{(a_2 + \alpha a_1)\,E_1F_1} + \frac{4a_1}{a_2 + \alpha a_1}\frac{P_0}{E_1F_1}\frac{a_2}{k_1}e^{-k_1\left(\frac{a_2t+x}{a_2} - \frac{L(a_1+a_2)}{a_2a_1} - \frac{2h}{a_2}\right)} + D. \tag{A21}$$

Now we can write the formula for the displacement in the region 5 (the force $P(t) = P_0 = \text{const}$.)

$$u_5(x,t)=\frac{4a_1P_0}{(a_2+\alpha a_1)E_1F_1}\left(a_2t-L\frac{a_2}{a_1}-h-\frac{Ma_2^2}{E_2F_2}\left[1-e^{-k_1\left(\frac{a_2t+x}{a_2}-\frac{L(a_1+a_2)}{a_1}-\frac{2h}{a_2}\right)}\right]\right). \quad \text{(A22)}$$

The formula for the displacement in the region VII is:

$$u_{VII}(x,t)=\frac{4a_1P_0}{(a_2+\alpha a_1)^2E_1F_1}(a_1a_2\alpha t-a_2\alpha L+a_1h\alpha+ha_2-2a_1\alpha h)$$

$$-\frac{8(a_1)^2(a_2)^2\alpha P_0}{(a_2+\alpha a_1)^2E_1F_1}\frac{M}{E_2F_2}\left[1-e^{-\frac{E_2F_2}{Ma_2}\left(\frac{a_2t-L}{a_2}-\frac{2h}{a_2}\right)}\right]. \quad \text{(A23)}$$

The formula for the displacement in the region XII is:

$$u_{XII}(x,t)=\frac{4a_1P_0h}{(a_2+\alpha a_1)E_1F_1}\left(1+\frac{a_1}{a_2}\right)-\frac{2A\alpha ha_1}{a_2}-\frac{2Aa_1\alpha}{k_1}\left(e^{-\frac{2h}{a_2}k_1}-1\right)$$

$$-\frac{4(a_1)^2\alpha P_0}{(a_2+\alpha a_1)E_1F_1}\frac{Ma_2}{E_2F_2}\left[1-e^{-\frac{E_2F_2}{Ma_2}\frac{2h}{a_2}}\right]-AZ\alpha(a_1t+x)\left(1+4e^{-k_1\left(t+\frac{x}{a_1}-\frac{2L}{a_1}-\frac{4h}{a_2}\right)}\right)$$

$$+6\alpha AZL+20\alpha AZh\frac{a_1}{a_2}+4AZL\alpha e^{-k_1\left(t+\frac{x}{a_1}-\frac{2L}{a_1}-\frac{4h}{a_2}\right)}-4AZL\alpha\frac{a_1}{a_2}e^{-k_1\left(t+\frac{x}{a_1}-\frac{2L}{a_1}-\frac{4h}{a_2}\right)}$$

$$+4AZL\alpha\frac{a_1}{a_2}+4Z\alpha\frac{a_1}{a_2}\left(1-e^{-k_1\left(t+\frac{x}{a_1}-\frac{2L}{a_1}-\frac{4h}{a_2}\right)}\right)\left(A\frac{a_2}{k_1}-AL-AL\frac{a_2}{a_1}-4Ah\right.$$

$$\left.-\frac{P_0a_1a_2\left(1-e^{-\frac{E_2F_2}{Ma_2}\frac{2h}{a_2}}\right)}{(a_2+\alpha a_1)E_1F_1k_1}\right)+A\alpha(a_1t+x)\left(1+4e^{-k_1\left(t+\frac{x}{a_1}-\frac{2L}{a_1}-\frac{4h}{a_2}\right)}\right)-6\alpha AL-20\alpha Ah\frac{a_1}{a_2}$$

$$-4AL\alpha e^{-k_1\left(t+\frac{x}{a_1}-\frac{2L}{a_1}-\frac{4h}{a_2}\right)}\left(1-\frac{a_1}{a_2}\right)-4AL\frac{a_1}{a_2}\alpha+4\frac{a_1}{a_2}\alpha\left(e^{-k_1\left(t+\frac{x}{a_1}-\frac{2L}{a_1}-\frac{4h}{a_2}\right)}-1\right)\left(A\frac{a_2}{k_1}-AL\right.$$

$$\left.-AL\frac{a_2}{a_1}-4Ah-\frac{P_0a_1a_2\left(1-e^{-\frac{E_2F_2}{Ma_2}\frac{2h}{a_2}}\right)}{(a_2+\alpha a_1)E_1F_1k_1}\right)$$

where

$$A = \frac{2P_0 a_1 (\alpha a_1 - a_2)}{E_1 F_1 (a_2 + \alpha a_1)^2} \quad \text{and} \quad Z = \frac{\alpha a_1 - a_2}{a_2 + \alpha a_1}. \tag{A24}$$

References

[1] Z. WESOŁOWSKI, *Akustyka ciała sprężystego* [in Polish], PWN, Warszawa 1989.

[2] F. LANZA DI SCALEA, R. E. GREEN Jr., *Experimental observation of the intrusive effect of a contact transducer on ultrasound propagation*, Ultrasonics, **37**, 179–183 (1999).

[3] D. M. NORRIS Jr., W. C. YOUNG, *Complex modulus measurement by longitudinal vibration testing, Experimental Mechanics*, **10**, 93–96 (1970).

[4] T. PRITZ, *Transfer function method for investigating the complex modulus of acoustical materials: rod like specimen,* Journal of Sound and Vibration **81**, 359–376 (1982).

[5] S. ÖDEEN, B. LUNDBERG, *Determination of complex modulus from measured end-point acceleration of an impacted rod specimen*, J. of Sound and Vibration, **165**(1), 1–8 (1993).

[6] C. BACON, J-L. LATAILLADE, *Development of the Kolsky-Hopkinson technics and applications for non-conventional testing*, 1–58, [in:] New experimental methods in material dynamics and impact, W. K. NOWACKI, J. R. KLEPACZKO [Eds.], IPPT PAN, 2001.

[7] C. BACON, B. HOSTEN, *Acoustic wave generation in viscoelastic rods by time-gated microwaves*, JASA, 106, 1, 195–201 (1999).

[8] C. BACON, E. GUILLIORIT, B. HOSTEN, D. E. CHIMENTI, *Acoustic wave generated by pulsed microwaves in viscoelastic rods: Modeling and experimental verification*, JASA, 110, 3, 1398–1407 (2001).

[9] B. POUET, N. RASOLOFOSAON, *Measurement of broadband intrinsic ultrasonic attenuation and dispersion in solids with laser techniques*, JASA 93, 1286–1292 (1993).

[10] H. KWUN, J. J. HANLEY, C. M. TELLER, *Performance of a noncontact magnetostrictive AE sensor on a steel rod*, J. of Acoustic Emission **11**, 1, 27–32 (1993).

[11] J. OSIECKI, *Reflection of a plane stress wave in a non-homogeneous solid medium*, Proceedings of Vibration Problems, **2**, 7, 155–178 (1961).

[12] A. VARY, *Ultrasonic measurement of material properties*, [in:] Research Techniques in NDT vol. IV, R. S. SHARPE [Ed.], 159–204 (1980).

[13] G. ŁYPACEWICZ, *Piezoelektryczne układy nadawczo-odbiorcze dla celów ultrasonografii* [in Polish], Prace IPPT PAN, 22/1995.